Backscatter Communication based Sensor Data Collection using LASER powered UAV

Amit Goel and Swades De
Bharti School of Telecommunication and Department of Electrical Engineering
Indian Institute of Technology Delhi, New Delhi 110016, India
E-mail: Amit.goel@dbst.iitd.ac.in, and swadesd@ee.iitd.ac.in

***Abstract*—The utility of unmanned aerial vehicle (UAV)-based data collection for massive sensor networks has received great attention. However, limited onboard battery capacity poses a constraint on its operation. In this paper, we model data collection of backscatter nodes using UAVs that are supported by wireless energy transfer from LASER based charging stations (LCS) for sustainable operations. Under the assumption that UAV to backscatter node channel experiences Nakagami-m fading, we derive the expression for signal-to-noise ratio (SNR). We define expressions for overall backscatter energy outage probability and overall backscatter SNR outage probability as the metrics of sustainable operations. Our numerical simulations reveal that, at optimal transmit power up to around 55$\%$ of UAV operations are reliable and completely sustainable via LCS.**

***Index Terms*—Aerial base station, backscatter communication, energy harvesting, free space optics (FSO), radio-frequency (RF) energy transfer, stochastic geometry**

I. Introduction

Wireless sensor networks (WSN) with conventional Internet of Things (IoT) nodes have high initial setup costs and high operation power requirements as well due to oscillators and other radio components. The scientific community has renewed interest in backscatter communication since it has been identified as the primary enabler of ultra-low power communication. In monostatic backscatter communication based architecture for e.g., RFID, backscatter receiver consist of onboard carrier emitter (CE). The CE generates an unmodulated signal which the backscatter tag modulates and reflects back to the backscatter receiver. In bistatic backscatter architecture, CE is dedicated, but CE and the backscatter receiver are physically separable. In ambient backscatter communication (amBc) there is no dedicated CE; rather, ambient RF signal sources are utilized as carrier signals, e.g., radio and cellular towers, etc. The authors in [1] considered UAV-based backscatter communication with multiple CE located on the ground and maximize the energy efficiency of the UAV while optimizing the node visiting sequence and CE's transmission power. However, in remote/rural areas, having terrestrial CEs with high density is less likely [2]. Therefore, UAV-based monostatic backscatter architectures are more preferred in such scenarios.

UAVs have been proposed as a component of future IoT networks, with the goal of connecting things under diverse circumstances and network conditions [3]. It is generally established that IoT devices are dispersed randomly throughout a large area of interest for different applications like environmental monitoring, etc. Due to their adaptability, interoperability, and cost-efficient operations, UAV-aided IoT systems are expected to considerably address coverage limitations in hostile settings. Additionally, UAVs' ability to operate at lower altitudes increases the probability of LoS connections between UAVs and terrestrial IoT devices, making them the perfect candidate to perform data collection processes [4].

Unmanned aerial vehicles (UAVs) also have the ability to alter their locations on the fly, which enables them to manage dense IoT deployment scenarios effectively. The authors in [5], presented a framework in which UAV was used to capture IoT data rapidly and efficiently, UAV trajectory was optimized while maximizing energy efficiency. The authors in [6], [7] utilized UAV to power IoT nodes for wireless energy transfer. In [8], for UAV-aided powering of IoT nodes a resource allocation strategy based on dynamic game theory was formulated. RF energy transfer channel model was studied in [9].

UAV-aided sensor data collection is appealing due to the UAV maneuverability, and backscatter based charging and data collection it is a key enabler of ultra-low power, low data rate, and sustainable WSN. However, limited onboard energy capacity imposes constraints on the operational capacity of UAVs. The UAV has to return to its base for offline charging purposes frequently. Compared to energy optimization and repeated offline charging of the UAV battery, free space optical link (FSO) based connectivity between the UAV and LASER based charging station (LCS) is a better alternative [10] for energy sustainability.

Inspired by the aforementioned advantages and challenges, in this paper we investigate the sustainability aspect of UAV-based backscatter sensor node data collection process aided by LCS. (1) We first derive a closed form expression of SNR outage probability of the backscattered signal received by the UAV from the backscatter node. (2) We utilize concepts of stochastic geometry and used the Poisson line cox process (PLCP) to model and study the impact of the presence of LCSs. (3) Furthermore, we derive overall backscatter energy outage probability and overall backscatter SNR outage probability and drew useful inferences related to the utility of LCS from the sustainable communication point of view.

II. System Model

In this section, the proposed architecture of the UAV-aided data collection process using the backscatter-based sensor node

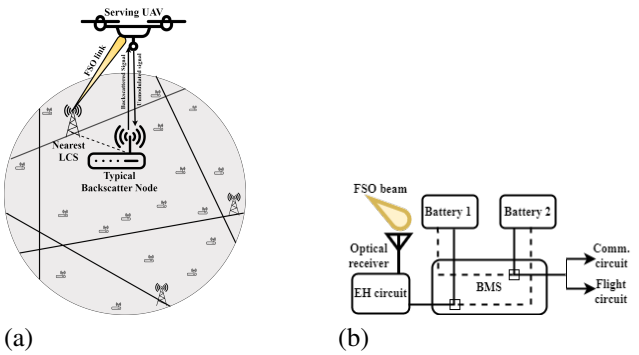

(a) (b)

Fig. 1. (a) Schematic for the LCS assisted UAV based data collection system consisting of multiple backscatter sensor nodes, UAV, LCSs deployed at the checkpoints on the roads passing through the region of interest. (b) EH mechanism at UAV.

communication, supported by LCS for sustainable operation, is presented.

Consider a scenario where backscatter sensor nodes are deployed to monitor the region of interest situated in a remote geographical location. Since the communication range of the nodes is limited, therefore, UAVs are utilized for data collection from backscatter nodes. UAVs have high flexibility in terms of mobility, but their operation time is constrained due to limited battery capacity. To eliminate this constraint, UAV's operations are supported by LCSs. LCSs are mounted at the checkpoints on the roads passing through the region of interest. We assume the checkpoints are connected to stable power sources to power LCS.

We assumed that backscatter nodes deployed in the region of interest are at the same height. The position of backscatter nodes (BSCN) are modeled as a 2D homogeneous Poisson point process (HPPP) Φ_B defined on R^2 with intensity λ_B. The position of LCSs are modeled via PLCP. In PLCP, the roads are modeled as a network of lines defined according to the Poisson line process (PLP) Φ_R. Using normal form representation of line in R^2, the following two parameters are required, ρ representing the perpendicular distance from origin, δ representing the angle between the perpendicular to the line from the origin and x-axis measured in an anti-clockwise manner. These parameters (ρ and δ) are generated via 2D HPPP with an intensity λ_R defined on $[0,2\pi) \times [0,\infty)$. Corresponding to every pair of parameters, a unique line is generated in R^2. The position of checkpoints on each road are modeled as 1D HPPP Φ_C with intensity λ_C. We refer to the overall process of LCS locations as Φ_{LCS}, which is defined as

$$\Phi_{LCS} = \cup_{r_i \in \Phi_R} \Phi_{C_{r_i}}, \tag{1}$$

which includes all the LCSs on all the roads. In this way, we transform location aspect of the proposed communication architecture into a stochastic geometry model.

As shown in Fig. 1, UAV maneuvers in the region of interest to carry out the data collection process. Consider a typical backscatter node located at the origin being served by the UAV. The UAV hovers over the backscatter node at a fixed height h_{UAV} for a total serving time T_s. The backscatter device utilizes a fraction of serving time T_s for energy harvesting T_{eh} and remaining time T_{com} for performing communication $T_s = T_{com} + T_{eh}$.

While hovering over the backscatter node, the UAV establishes an FSO link with the nearest LCS. LCS comprise of an optical transmitter that emits a focused optical beam with constant power towards the UAV. The optical receiver mounted on the UAV harvests energy from the optical beam impinging on the receiver surface. We consider that UAV is equipped with two separate batteries managed by an intelligent battery management system (BMS), such that while one of them is being charged via received power from the LCS, the other battery is utilized to carry out UAV operations (flight and data collection) [11]. Since the associated LCS transmit signals at a different spectrum range (1510 nm wavelength), there is no self-interference between (LCS to UAV) and (UAV to BSCN) links. It is considered that UAV has sufficient memory to store the total data collected from the backscatter nodes; therefore, the backhaul connectivity for data transmission is not required.

During time period T_{com}, T_{eh} the UAV transmits fixed continuous wave signal with power P^d_{tx}, P^e_{tx} respectively. Therefore, during T_{com}, T_{eh} power consumption of UAV is $P_{flight} + P^d_{tx}$, $P_{flight} + P^e_{tx}$ respectively, where P_{flight} is the power consumed in flight operations. We assume that the amount of energy harvested during backscatter communication is very less and, therefore, can be neglected. Communication will be carried out if and only if the backscatter node harvests sufficient energy during energy harvesting phase. We assumed that sensor nodes have renewable energy-based battery recharging mechanism to carry out sensing operations, and thus the RF energy received is utilized only for up-link data transfer.

III. Statistical Modeling of LCS to UAV and UAV to Backscatter Node Communication Links

In this section, we first define the wireless channel link between LCS and UAV and between UAV and backscatter nodes. Thereafter, we mathematically express the effect of separation distance and fading coefficient over received power, and finally, we derive the expression of overall backscatter SNR and energy outage probability.

A. Channel modeling for backscatter communication

During the communication time backscatter device modulates the incident signal via a factor known as the reflection coefficient denoted by β where β lies between zero and one. In the proposed system, the communication between the UAV and backscatter-based sensor node is governed by monostatic backscatter communication (mBC) mechanism. In mBC system, UAV first transmits an unmodulated signal to the backscatter device x_1. The signal received by the backscatter device is given by

$$y_B = h_{U-B}\sqrt{P^d_{tx}}x_1 + w_1. \tag{2}$$

The backscatter node modulates the received signal according to the information signal x_2, and reflect back the modulated signal. The received signal by UAV is given by

$$y_U = \sqrt{\beta} h_{B-U} h_{U-B} \sqrt{P_{tx}^d} x_1 x_2 + h_{B-U} w_1 + w_2, \quad (3)$$

where P_{tx}^d is the transmit power of the UAV during the time of data collection, w_1 and w_2 denotes additive white Gaussian noise (AWGN). Since the UAV is hovering above the backscatter node, we considered that the channel link is LOS dominated. The channel gain $h_{U-B} = \sqrt{G_{tx} G_{bsc} (\lambda/4\pi)^2 d^{-\eta}} \tilde{h}_{U-B}$ and, $h_{B-U} = \sqrt{G_{bsc} G_{rx} (\lambda/4\pi)^2 d^{-\eta}} \tilde{h}_{U-B}$ in (3) are influenced by both path loss and small scale fading, where $\tilde{h}_{U-B}$ and, $\tilde{h}_{B-U}$ denotes small-scale fading coefficient in uplink and downlink and are modeled as identical and independent Nakagami-m distributed [12], d denotes distance between UAV and backscatter node, G_{tx}, G_{rx} and G_{bsc} denotes transmitter, receiver and backscatter node antenna gain, η denotes path loss exponent and $\lambda (= c/f_c)$ denotes wavelength of transmit signal by UAV. The SNR of the received signal is expressed as

$$SNR = \frac{\beta P_{tx}^d \left| h_{U-B} \right|^2 \left| h_{B-U} \right|^2}{\sigma_1^2 \left| h_{B-U} \right|^2 + \sigma_2^2}, \quad (4)$$

where σ_1^2 and σ_2^2 denotes noise power. The closed form expression for the cumulative distribution function (CDF) of SNR evaluated at SNR threshold x, given that the transmitted power is P_{tx}^d is expressed as

$$F_{SNR}(x)|_{P_{tx}^d} = \frac{1}{\Gamma m_2} \left[1 - \exp\left(-\frac{m_1 x}{Z_1} \right) \sum_{k=0}^{m_1 - 1} \left(\frac{m_1 x}{Z_1} \right)^k \times \frac{1}{k!} \sum_{i=0}^{k} \binom{k}{i} \left(\frac{C}{Z_2} \right)^i m_2^i G_{0,2}^{2,0} \left(\begin{matrix} 1 - m_2 + i, 1 \\ - \end{matrix} \middle| \frac{Z_1 Z_2}{m_1 C x} \right) \right]. \quad (5)$$

Proof. See Appendix A. ■

Backscatter SNR outage is defined as the probability that the received SNR is below certain threshold γ_{th}^{SNR}, given that UAV transmit power is P_{tx}^d. Mathematically it is expressed as

$$\mathbb{P}_{out}^{B,snr} \left(\gamma_{th}^{SNR} \right) \Big|_{P_{tx}^d} = F_{SNR} \left(\gamma_{th}^{SNR} \right) \Big|_{P_{tx}^d}. \quad (6)$$

B. Energy harvesting by backscatter nodes

During the energy harvesting phase, let P_{rx}^B denotes the received power at backscatter node. Since the energy harvesting is not efficient, therefore, the harvested power given that received power is P_{rx}^B is given by [13]

$$P_{EH}^B \left(P_{rx}^B \right) = \frac{P_m}{e^{(-\upsilon P_0 + \vartheta)}} \left\{ \frac{1 + e^{(-\upsilon P_0 + \vartheta)}}{1 + e^{(-\upsilon P_{rx}^B + \vartheta)}} - 1 \right\}, \quad (7)$$

where P_m denotes maximum possible harvest power, P_0 denotes receiver sensitivity, υ and ϑ are shaping parameters. If the energy harvesting operation is carried out for time period of T_{eh} then the total energy harvested is expressed as

$$E^B \left(P_{tx}^e \right) = T_{eh} * P_{EH}^B \left(P_{rx}^B \right), \quad (8)$$

where $P_{rx}^B = \left| \tilde{h}_{U-B} \right|^2 G_{tx} G_{bsc} \left(\lambda/4\pi \right)^2 d^{-\eta} P_{tx}^e$ Let P_c denotes the minimum required power for circuit operation while backscatter communication is taking place. Therefore, the minimum energy required to be harvested beforehand for T_{com} communication time is $E_{req} = P_c \times T_{com}$. **Backscatter energy outage** occurs when the energy harvested $E^B \left(P_{tx}^e \right)$ by backscatter device is less than E_{req}. Mathematically it is expressed as

$$\mathbb{P}_{out}^{B,eh} \left(P_{tx}^e \right) = \mathbb{P} \left(E^B \left(P_{tx}^e \right) < E_{req} \right).$$

Using (7) the above expression reduces to

$$\mathbb{P}_{out}^{B,eh} \left(P_{tx}^e \right) = F_{|h_{U-B}|^2}(K), \quad (9)$$

where

$$K = \left(\vartheta - \log \left(\frac{(T_{eh} P_m - P_c T_{com}) e^{(-\upsilon P_0 + \vartheta)}}{P_c T_{com} e^{(-\upsilon P_0 + \vartheta)} + T_{eh} P_m} \right) \right) \times \frac{1}{\upsilon G_{tx} G_{bc} \left(\lambda/4\pi \right)^2 d^{-\eta} P_{tx}^e}.$$

C. Energy harvesting by UAV from LCS

In this paper we consider that UAV is linked with LCS based on nearest LCS association policy. Let d_{min} denotes the distance between the projection of UAV on R^2 plane and nearest LCS. The CDF, $F_{d_{min}}(\ell)$ [14] and probability density function (PDF) $f_{d_{min}}(\ell)$ at $d_{min} = \ell$ are expressed as

$$F_{d_{min}}(\ell) = 1 - e^{\left(-2\pi\lambda_R \int_{r=0}^{\ell} 1 - \exp\left(-2\lambda_C \sqrt{\ell^2 - r^2} \right) dr \right)}, \quad (10)$$

$$f_{d_{min}}(\ell) = \left(2\pi^2 \lambda_R \lambda_C \ell \left[I_0 \left(-2\ell\lambda_C \right) + L_0 \left(-2\ell\lambda_C \right) \right] \right) \times \left[\exp\left(\pi^2 \lambda_R \ell \left[L_1 \left(-2\ell\lambda_C \right) + I_1 \left(-2\ell\lambda_C \right) \right] \right) \right], \quad (11)$$

Proof. $f_{d_{min}}(\ell)$ is derived in similar fashion to [15] with detailed procedure given in Appendix B. ■

Let $z = \sqrt{h_{UAV}^2 + \ell^2}$ denotes the distance between the UAV and nearest LCS, then the received power from the nearest LCS is given by [16]

$$P_{rx}^{LCS} = \frac{\Omega \Lambda \xi P_{tx}^{LCS} \exp(-\varphi z) h_t}{\left(\Delta + z\Theta \right)^2}, \quad (12)$$

where h_t represents turbulence effect which follows gamma gamma distribution. The PDF of h_t is expressed as

$$f_{h_t}(x) = \frac{2(\alpha_t \beta_t)^{\frac{\alpha_t + \beta_t}{2}} - 1}{\Gamma \alpha_t \Gamma \beta_t} x^{\frac{\alpha_t + \beta_t}{2} - 1} \kappa_{\alpha_t - \beta_t} \left[2\sqrt{\alpha_t \beta_t x} \right], \quad (13)$$

where Ω denotes the energy harvesting efficiency, Λ denotes area of the receiver at UAV, ξ denotes combined transmitter receiver optical efficiency, P_{tx}^{LCS} denotes the transmit power of LCS, φ denotes attenuation factor, Δ denotes initial laser beam size, Θ denotes angular spread of laser beam, α_t and β_t are turbulence parameters.

Let $\varsigma_{th,i}$ denotes the power consumed at an instance where $i \in \{E, D\}$ such that $\varsigma_{th,E} = \left(P_{flight} + P_{tx}^e \right)$ and $\varsigma_{th,D} = \left(P_{flight} + P_{tx}^d \right)$.

UAV power reception probability is defined as the probability of harvesting P_{rx}^{UAV} amount of power via FSO link from nearest LCS. Mathematically it is expressed as

$$\mathbb{P}\left(P_{rx}^{UAV} > \varsigma_{th,i}\right)|_z = 1 - F_{P_{rx}^{UAV}}\left(\varsigma_{th,i}, z\right),$$

where

$$F_{P_{rx}^{UAV}}\left(\varsigma_{th,i}, z\right) = F_{h_t}\left(\frac{\varsigma_{th,i}\left(\Delta + z\Theta\right)^2}{\Omega\Lambda\xi P_{tx}^{LCS}\exp(-\varphi z)}\right).$$

Using (11) finally we have

$$\mathbb{P}\left(P_{rx}^{UAV} > \varsigma_{th,i}\right) = 1 - \int_0^\infty F_{P_{rx}^{UAV}}\left(\varsigma_{th,i}, z\right) f_{d_{min}}(\ell) d\ell. \tag{14}$$

D. Overall outage probability

Provided that P_{flight} is known and constant. With UAV transmission power P_{tx}^e, during energy harvesting time period **overall backscatter energy outage probability** ($\mathbb{P}_E^{out}$) is defined as the probability with which either power received from LCS is less than $P_{flight} + P_{tx}^e$ or harvested power at backscatter node is less than $P_{req}\left(= \frac{P_C T_{com}}{T_{eh}}\right)$. With UAV transmission power P_{tx}^d. During data transmission operation time period **overall backscatter SNR outage probability** ($\mathbb{P}_D^{out}$) is defined as the probability with which either the power received from LCS is less than $P_{flight} + P_{tx}^d$ or received SNR at UAV is less than the defined SNR threshold value.

Using the above two definition, system outage probability is defined as

$$\mathbb{P}_{out}^{sys} = \frac{T_{com}}{T_{com} + T_{eh}}\mathbb{P}_E^{out} + \frac{T_{eh}}{T_{com} + T_{eh}}\mathbb{P}_D^{out}, \tag{15}$$

where

$$\begin{aligned}\mathbb{P}_E^{out} &= \mathbb{P}\left(P_{rx}^{UAV} < P_{flight} + P_{tx}^e\right) + \\ &\mathbb{P}\left(P_{rx}^{UAV} > P_{flight} + P_{tx}^e\right) \times \mathbb{P}\left(P_{EH}^B\left(P_{tx}^e\right) < P_{req}\right) \\ &= 1 - \left[1 - \mathbb{P}_{out}^U\left(\varsigma_{th,E}\right)\right]\left[1 - \mathbb{P}_{out}^{B,eh}\left(P_{tx}^e\right)\right]. \end{aligned} \tag{16}$$

Similarly,

$$\begin{aligned}\mathbb{P}_D^{out} &= \mathbb{P}\left(P_{rx}^{UAV} < P_{flight} + P_{tx}^d\right) + \\ &\mathbb{P}\left(P_{rx}^{UAV} > P_{flight} + P_{tx}^d\right) \times \mathbb{P}\left(SNR\left(P_{tx}^d\right) < \gamma_{th}^{SNR}\right) \\ &= 1 - \left[1 - \mathbb{P}_{out}^U\left(\varsigma_{th,D}\right)\right]\left[1 - \mathbb{P}_{out}^{B,snr}\left(\gamma_{th}^{SNR}\right)\Big|_{P_{tx}^d}\right]. \end{aligned} \tag{17}$$

IV. Results and Discussion

In this section, we present the analytical and simulation-based results generated using MATLAB to validate our proposed framework. The values of the simulation set-up parameters are listed in Table I.

Fig. 2 shows the data reception quality for the proposed framework for both theoretical and simulation-based scenarios. The simulation results are obtained using Monte Carlo simulations. The variation of SNR outage probability with transmission power is plotted at different SNR threshold values.

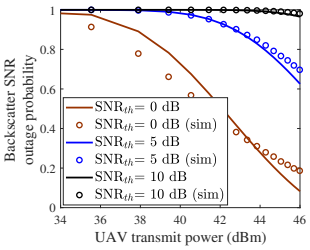

Fig. 2. SNR outage probability of backscatter node.

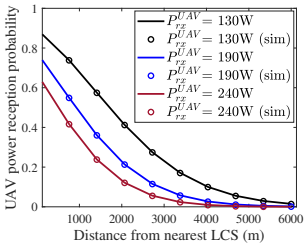

Fig. 3. LCS to UAV power reception probability.

Fig. 3 and 4 showcase the uninterrupted operation capacity of the proposed framework. Fig. 3 shows the LCS to UAV power reception probability, while Fig. 4 shows the variation of UAV power reception probability for different LCS densities. Fig. 5 and 6 showcase the overall SNR outage probability at given UAV transmit power for different SNR threshold values and the energy outage probability at given UAV transmit power for varying values of LCS density, respectively.

We know that the higher the transmission power, the lower the likelihood of an outage. This pattern can be observed in Fig. 5 where with an increase in UAV transmission power, there is a decline in outage probability until it reaches an inflection point. Beyond this inflection point, as we further increase the transmission power, the outage probability starts rising again. The reason being with a further increase in UAV transmit power, the total power requirement increases, and the chances of receiving more power from the associated LCS decreases (as can be seen from Fig. 3). Therefore from Fig. 5 and 6, we can conclude that with road density λ_R = 0.57 Km^{-1} and checkpoint density λ_c = 0.5 Km^{-1}, approx. 55 percent of the time, the UAV total power consumption is supplied from LCS and the received SNR at the UAV is above the 0 dB. Therefore, compared to standalone UAV architecture, LCS-aided UAV-based data collection can serve more users with high reliability. Due to space constraints, resource allocation scheme description and detailed comparison will be presented in our future work.

In the wireless energy transfer based recharging process, the overall backscatter energy outage with the change in UAV transmission power is plotted in Fig. 6. We observe

TABLE I
Simulation parameters and values [13] [17] [18]

Parameter	Value	Parameter	Value
T_{com}	10 s	G_{bc}	0 dBi
T_{eh}	600 s	f_c	915 MHz
h_{UAV}	30 m	P_C	10.6 μW
P_{flight}	168 W	α_t , β_t	5.76, 3.6
σ_1^2, σ_2^2	1×10^{-9}	P_{tx}^{LCS}	1000 W
m_1, m_2	2	η	2
υ , ϑ	274 , 0.29	$\Omega\Lambda\xi$	0.004 m^2
P_m	0.00493 W	φ	10^{-6} m
P_0	0.000064 W	Δ	0.1 m
G_{tx}, G_{rx}	10 dBi	Θ	3.4×10^{-5}

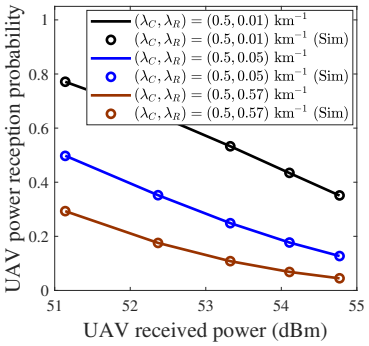

Fig. 4. UAV power reception probability at different densities of LCS.

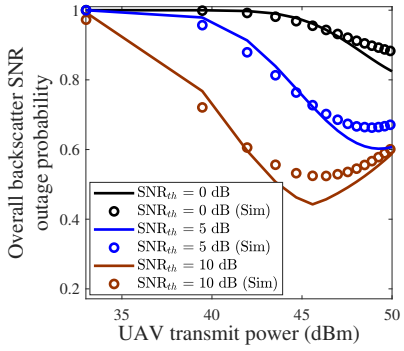

Fig. 5. Overall backscatter SNR outage probability at $\lambda_C = 0.5$ Km^{-1} $\lambda_R = 0.57$ Km^{-1}.

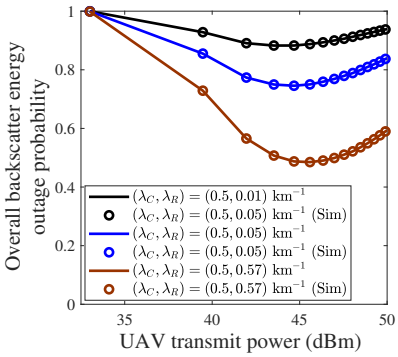

Fig. 6. Overall backscatter energy outage probability at different densities of LCS.

that, initially with an increase in transmission power the outage reduces. Once the inflection point is reached, the outage probability starts rising. At different LCS densities, the inflection point is achieved at different UAV transmission power. At higher densities, the distance between the UAV and the associated LCS decreases, and hence the chances of an outage get reduced.

V. Conclusion

In this paper, we have analyzed the UAV-assisted backscatter sensor node data collection. A closed-form expression for the backscatter SNR outage is derived. The scope of sustainable data collection process with UAV powered by the wireless energy transfer from the nearest LCS is evaluated using stochastic geometry. Expressions for the overall backscatter SNR outage and overall backscatter energy outage are derived by taking channel fading parameters and the nearest LCS distance. The constraint of backhaul link for sustainable communication can be incorporated as a possible extension of this study, which is left as a future work.

VI. Acknowledgement

This work was supported in part by the Science and Engineering Board, Department of Science and Technology (DST), Government of India, under Grant CRG/2019/002293; in part by the Indian National Academy of Engineering (INAE) through the Abdul Kalam Technology Innovation National Fellowship and by the Prime Minister Research Fellowship (PMRF).

Appendix

A. Proof of (5)

From (4) we have

$$SNR = \frac{\beta P_{tx}^d H_1 H_2 Y_1 Y_2}{H_2 Y_2 + C}, \tag{A.1}$$

where $H_1 = \epsilon_1/\sigma_1^2$, $H_2 = \epsilon_2/\sigma_2^2$, $\epsilon_1 = G_{tx}G_{bsc}(\lambda/4\pi)^2 d^{-\eta}$, $\epsilon_2 = G_{bsc}G_{rx}(\lambda/4\pi)^2 d^{-\eta}$, $d = h_{UAV}$ (since UAV is hovering above the typical backscatter node), $Y_1 = \left|\tilde{h}_{U-B}\right|^2$ and $Y_2 = \left|\tilde{h}_{B-U}\right|^2$. Since $\tilde{h}_{U-B}$, $\tilde{h}_{B-U}$ are Nakagami-m distributed therefore, $Y_1 \sim$ Gamma $(m_1, 1/m_1)$, $Y_1 \sim$ Gamma $(m_2, 1/m_2)$. Consequently, (A.1) we have

$$SNR = \frac{Z_1 Z_2 Y_1 Y_2}{Z_2 Y_2 + C}, \tag{A.2}$$

where $Z_1 = \beta P_{tx}^d \epsilon_1/\sigma_1^2$, $Z_2 = \epsilon_2/\sigma_2^2$, $C = 1/\sigma_2^2$. For Y_i, PDF $f_{Y_i}(x)$ and CDF $F_{Y_i}(x)$ are expressed as $f_{Y_i}(x) = \frac{m_i^{m_i}}{\Gamma m_i} x^{m_i - 1} e^{-m_i x}$, $F_{Y_i}(x) = \frac{1}{\Gamma m_i}\gamma(m_i, m_i x)$; $\forall i \in \{1, 2\}$. Backscatter SNR outage probability can be calculated as

$$\mathbb{P}(SNR < x) = \mathbb{P}\left(Y_1 < \frac{x}{Z_1}\left(1 + \frac{C}{Z_2 Y_2}\right)\right), \tag{A.3}$$

$$F_{SNR}(x) = \int_0^\infty \frac{1}{\Gamma m_i}\gamma\left(m_1, \frac{m_1 x}{Z_1}\left\{1 + \frac{C}{Z_2 y}\right\}\right) \times \frac{m_2^{m_2}}{\Gamma m_2} y^{m_2 - 1}\exp(-m_2 y)\mathrm{d}y. \tag{A.4}$$

Using [19, Eq. (8.352.1)], we have

$$\gamma\left(m_1, \frac{m_1 x}{Z_1}\left\{1 + \frac{C}{Z_2 y}\right\}\right) = (m_1 - 1)! \times \left(1 - \exp\left(-\frac{m_1 x}{Z_1}\left\{1 + \frac{C}{Z_2 y}\right\}\right) \times \left(\sum_{m=0}^{m_1 - 1} \frac{\left(\frac{m_1 x}{Z_1}\left\{1 + \frac{C}{Z_2 y}\right\}\right)^m}{m!}\right)\right), \tag{A.5}$$

Using binomial series expansion the following term can be written as

$$\left(1 + \frac{C}{Z_2 y}\right)^m = \sum_{i=0}^{m}\binom{m}{i}\left(\frac{C}{Z_2 y}\right)^i y^{-i}. \tag{A.6}$$

Thereafter, substituting (A.5), (A.6) in (A.4) we have

$$F_{SNR}(x) = \frac{m_2^{m_2}}{m_1! m_2!}(m_1-1)! \int_0^\infty f_{\gamma_2}(y)dy - \exp\left(-\frac{m_1 x}{Z_1}\right) \cdot \sum_{k=0}^{m_1-1} \left(\frac{m_1 x}{Z_1}\right)^k \frac{1}{k!} \sum_{i=0}^{k} \binom{k}{i} \left(\frac{C}{Z_2}\right)^i \times \int_0^\infty y^{m_2-i-1} \exp\left(-\frac{m_1 x C}{Z_1 Z_2 y}\right) \exp(-m_2 y)\mathrm{dy}. \quad \text{(A.7)}$$

The exponential terms of (A.7) can be expressed in terms of the Meijer-G function as

$$\exp(-m_2 y) = G_{0,1}^{1,0}\left(\begin{matrix} - \\ 0 \end{matrix}\middle| \, m_2 y\right), \exp\left(-\tfrac{m_1 x C}{Z_1 Z_2 y}\right) = G_{1,0}^{0,1}\left(\begin{matrix} 1 \\ - \end{matrix}\middle| \, \tfrac{Z_1 Z_2 y}{m_1 x C}\right),$$

where the Meijer-G function $G_{p,q}^{m,n}\left(\begin{matrix} a \\ b \end{matrix}\middle| \, Arg\right)$ is defined in [19, Eq. (9.301)]. Let

$$I_1 = \int_0^\infty y^{m_2-i-1} G_{0,1}^{1,0}\left(\begin{matrix} - \\ 0 \end{matrix}\middle| \, m_2 y\right) G_{1,0}^{0,1}\left(\begin{matrix} 1 \\ - \end{matrix}\middle| \, \frac{Z_1 Z_2 y}{m_1 x C}\right) \mathrm{dy}, \quad \text{(A.8)}$$

using [20, Eq. (07.34.21.0088.01)], I_1 can be expressed as

$$I_1 = m_2^{m_2-i} G_{2,0}^{0,2}\left(\begin{matrix} 1-m_2+i, 1 \\ - \end{matrix}\middle| \, \frac{Z_1 Z_2}{m_1 C x}\right). \quad \text{(A.9)}$$

Substituting (A.9) in (A.7), the CDF of SNR is expressed as

$$F_{SNR}(x) = \frac{1}{\Gamma m_2}\left[1 - \exp\left(-\frac{m_1 x}{Z_1}\right) \sum_{k=0}^{m_1-1} \left(\frac{m_1 x}{Z_1}\right)^k \times \frac{1}{k!} \sum_{i=0}^{k} \binom{k}{i} \left(\frac{C}{Z_2}\right)^i m_2^i G_{2,0}^{0,2}\left(\begin{matrix} 1-m_2+i, 1 \\ - \end{matrix}\middle| \, \frac{Z_1 Z_2}{m_1 C x}\right)\right]. \quad \text{(A.10)}$$

B. Proof of (11)

$f_{d_{min}}(\ell)$ is obtained by differentiating $F_{d_{min}}(\ell)$ in (10) using Leibniz integral rule. Thereby, $f_{d_{min}}(\ell)$ can be expressed as

$$f_{d_{min}}(\ell) = \left[4\pi\lambda_R\lambda_C \int_0^\ell \frac{\ell e^{-2\lambda_C\sqrt{\ell^2-r^2}}}{\sqrt{\ell^2-r^2}} dr\right][1 - F_{d_{min}}(\ell)]. \quad \text{(B.1)}$$

Let $\mathbb{I}_1 = \int_0^\ell \frac{\ell e^{-2\lambda_C\sqrt{\ell^2-r^2}}}{\sqrt{\ell^2-r^2}} d\ell$, substituting $\sqrt{\ell^2-r^2} = a$ and rearranging the terms, the expression reduces to $\mathbb{I}_1 = \int_0^\ell \ell e^{-2\lambda_C a}\left(\ell^2-a^2\right)^{-\frac{1}{2}}$ da. Using [19, Eq. (3.384.5)] $\mathbb{I}_1$ can be expressed as

$$\mathbb{I}_1 = \frac{\ell\sqrt{\pi}\Gamma(1/2)}{2}\left[I_o(-2\ell\lambda_C) + L_0(-2\ell\lambda_C)\right]. \quad \text{(B.2)}$$

Let $\mathbb{I}_2 = \mathbb{I}_{21} - \mathbb{I}_{22} = \int_{r=0}^{\ell} dr - \int_{r=0}^{\ell} exp\left(-2\lambda_C\sqrt{\ell^2-r^2}\right)$ dr, in I_{22} substituting $\sqrt{\ell^2-r^2} = b$ and rearranging the terms, we have $\mathbb{I}_{22} = \int_0^\ell b e^{-2\lambda_C b}\left(\ell^2-b^2\right)^{-\frac{1}{2}}$ db. Further, using [19, Eq. (3.389.3)], $\mathbb{I}_{22}$ can be written as

$$\mathbb{I}_{22} = \ell + \frac{\ell\sqrt{\pi}\Gamma(1/2)}{2}\left[I_1(-2\ell\lambda_C) + L_1(-2\ell\lambda_C)\right], \quad \text{(B.3)}$$

where $I_0(x), I_1(x)$ represents modified Bessel functions of the first kind and $L_0(x), L_1(x)$ represents the modified Struve functions.

Further, substituting (B.2) and (B.3), the integral in (B.1) can be expressed as

$$f_{d_{min}}(\ell) = \left(2\pi^2\lambda_R\lambda_C\ell\left[I_0(-2\ell\lambda_C) + L_0(-2\ell\lambda_C)\right]\right) \times \left[\exp\left(\pi^2\lambda_R\ell\left[L_1(-2\ell\lambda_C) + I_1(-2\ell\lambda_C)\right]\right)\right]. \quad \text{(B.4)}$$

REFERENCES

[1] G. Yang, R. Dai, and Y.-C. Liang, "Energy-efficient UAV backscatter communication with joint trajectory design and resource optimization," *IEEE Trans. Wireless Commun.*, vol. 20, no. 2, pp. 926–941, 2020.

[2] M. Hua, L. Yang, C. Li, Q. Wu, and A. L. Swindlehurst, "Throughput maximization for UAV-aided backscatter communication networks," *IEEE Trans. Commun.*, vol. 68, no. 2, pp. 1254–1270, 2019.

[3] Y. Zeng, J. Lyu, and R. Zhang, "Cellular-connected UAV: Potential, challenges, and promising technologies," *IEEE Wireless Commun.*, vol. 26, no. 1, pp. 120–127, 2018.

[4] M. M. Azari, F. Rosas, K.-C. Chen, and S. Pollin, "Ultra reliable UAV communication using altitude and cooperation diversity," *IEEE Trans. Commun.*, vol. 66, no. 1, pp. 330–344, 2017.

[5] X. Liu, Y. Liu, N. Zhang, W. Wu, and A. Liu, "Optimizing trajectory of unmanned aerial vehicles for efficient data acquisition: A matrix completion approach," *IEEE Internet Things J.*, vol. 6, no. 2, pp. 1829–1840, 2019.

[6] S. Suman, S. Kumar, and S. De, "Path loss model for UAV-assisted RFET," *IEEE Commun. Lett.*, vol. 22, no. 10, pp. 2048–2051, 2018.

[7] S. Suman and S. Kumar and S. De, "UAV-assisted RFET: A novel framework for sustainable WSN," *IEEE Trans. Green Commun. Netw.*, vol. 3, no. 4, pp. 1117–1131, 2019.

[8] B. Liu, H. Xu, and X. Zhou, "Resource allocation in unmanned aerial vehicle (UAV)-assisted wireless-powered internet of things," *IEEE Sensors J.*, vol. 19, no. 8, p. 1908, 2019.

[9] S. Kumar, S. De, and D. Mishra, "RF energy transfer channel models for sustainable IoT," *IEEE Internet of Things J.*, vol. 5, no. 4, pp. 2817–2828, 2018.

[10] D. Wu, X. Sun, and N. Ansari, "An FSO-based drone charging system for emergency communications," *IEEE Trans. Veh. Technol.*, vol. 69, no. 12, pp. 16 155–16 162, 2020.

[11] X. Liu and N. Ansari, "Toward green IoT: Energy solutions and key challenges," *IEEE Commun. Mag.*, vol. 57, no. 3, pp. 104–110, 2019.

[12] H. Liu, S.-J. Yoo, and K. S. Kwak, "Opportunistic relaying for low-altitude UAV swarm secure communications with multiple eavesdroppers," *J. Commun. Netw.*, vol. 20, no. 5, pp. 496–508, 2018.

[13] S. Wang, M. Xia, K. Huang, and Y.-C. Wu, "Wirelessly powered two-way communication with nonlinear energy harvesting model: Rate regions under fixed and mobile relay," *IEEE Trans. Wireless Commun.*, vol. 16, no. 12, pp. 8190–8204, 2017.

[14] G. Ghatak, A. De Domenico, and M. Coupechoux, "Small cell deployment along roads: Coverage analysis and slice-aware RAT selection," *IEEE Trans. Commun.*, vol. 67, no. 8, pp. 5875–5891, 2019.

[15] M. N. Sial, Y. Deng, J. Ahmed, A. Nallanathan, and M. Dohler, "Stochastic geometry modeling of cellular V2X communication over shared channels," *IEEE Trans. Veh. Technol.*, vol. 68, no. 12, pp. 11 873–11 887, 2019.

[16] D. Killinger, "Free space optics for laser communication through the air," *Opt. Photon. News*, vol. 13, no. 10, pp. 36–42, Oct 2002.

[17] T. Zhang, G. Liu, H. Zhang, W. Kang, G. K. Karagiannidis, and A. Nallanathan, "Energy-efficient resource allocation and trajectory design for UAV relaying systems," *IEEE Trans. Commun.*, vol. 68, no. 10, pp. 6483–6498, 2020.

[18] A. Ranjha and G. Kaddoum, "URLLC-enabled by laser powered UAV relay: A quasi-optimal design of resource allocation, trajectory planning and energy harvesting," *IEEE Trans. Veh. Technol.*, vol. 71, no. 1, pp. 753–765, 2021.

[19] I. S. Gradshteyn and I. M. Ryzhik, "Table of integrals, series and products," *New York, NY, USA: Academic*, 2000.

[20] I. Wolfram, "Wolfram, research, mathematica edition: Version 10.0. champaign," *Wolfram Research, Inc.*, 2010.